Terahertz radiation enhancement in dipole photoconductive antenna on LT-GaAs using a gold plasmonic nanodisk array

Bashirpour, Mohammad; Poursafar, Jafar; Kolahdouz, Mohammadreza; Hajari, Mohsen; Forouzmehr, Matin; Neshat, Mohammad; Hajihoseini, Hamid; Fathipour, Morteza; Kolahdouz, Zahra; Zhang, Guoqi

DOI
10.1016/j.optlastec.2019.105726

Publication date
2019

Document Version
Final published version

Published in
Optics and Laser Technology

Optics and Laser Technology 120 (2019) 105726

Contents lists available at ScienceDirect

Optics and Laser Technology

journal homepage: www.elsevier.com/locate/optlastec

Full length article

Terahertz radiation enhancement in dipole photoconductive antenna on LT-GaAs using a gold plasmonic nanodisk array

Mohammad Bashirpour[a], Jafar Poursafar[a], Mohammadreza Kolahdouz[a,*], Mohsen Hajari[a], Matin Forouzmehr[a], Mohammad Neshat[a], Hamid Hajihoseini[b], Morteza Fathipour[a], Zahra Kolahdouz[c,*], Guoqi Zhang[c]

[a] School of Electrical and Computer Engineering, Faculty of Engineering, University of Tehran, Tehran
[b] Science Institute, University of Iceland, Dunhaga 3, IS-107 Reykjavik, Iceland
[c] Delft Institute of Microsystems and Nanoelectronics (DIMES-EKL), Delft University of Technology, Delft 2628CT, the Netherlands

HIGHLIGHTS

- A plasmonic THz PCA consisting Ti/Au nanodisks in the antenna gap is presented.
- All structural parameters were optimized to reach highest electron-hole generation.
- The PCA benefits from enhanced quantum efficiency enabled by plasmon excitation.
- The finalized PCA resulted in more than 5.6 times THz electric field radiation.
- This THz field enhancement shows a way to improve the optical-to-THz efficiency.

ABSTRACT

This study proposes a new-fashioned plasmonic photoconductive antenna (PCA) with high optical-to-terahertz (THz) conversion efficiency. Finite element method was used to investigate and optimize the interaction of 800 nm femtosecond laser with the designed nanodisk array in the antenna's gap using its geometrical parameters. According to the simulation results, our optimized nanoplasmonic structure showed more than 38% enhancement in the absorption efficiency compared to the conventional structure without any nanostructure. Measuring the THz radiation of the fabricated PCAs using a time domain spectroscopy setup exhibited an exceptional 5.6 times higher electric field in 0.1–2.5 THz range compared to a similar PCA but without nanoplasmonic structure.

1. Introduction

One promising method for terahertz wave generation is based on photoconductive emitters, where, a femtosecond laser pulse illumination on a biased gap of a PCA generates a transient photocurrent by drifting electron-hole pairs between the electrodes. According to the Maxwell's wave equations, a transient photocurrent with a sub-picosecond pulse width results in a THz electromagnetic wave [1–3]. The compact design, room temperature operation, low cost and broadband radiation have made PCAs, good candidates for THz generation and detection in a wide range of applications, such as environmental monitoring, astronomy, bio imaging, security screening, molecular spectroscopy, and many others [2,4]. Despite all advantages, conventional PCAs acquire low optical-to-THz conversion efficiencies of 0.01% to 0.1% for the input laser power of 1–50 mW that limits the application of these devices [5,6]. Lots of efforts have been used to overcome this limitation [7–9].

Recently, plasmonic and dielectric nanostructures have been employed to manipulate the optical wave and enhance the efficiency of THz PCAs [10–14]. Nanoplasmonic structures result in scattering of the femtosecond laser pulse and thereby its coupling into the low temperature grown-GaAs (LT-GaAs). This phenomenon occurs through different schemes such as light scattering, localized surface plasmons, and surface plasmon polariton [15–20]. This process enhances the optical pump intensity, the local field, and the photo-generated carrier concentration near the surface of the LT-GaAs layer. Thus, it generates a higher transient photocurrent in the PCA gap. This leads to significantly higher THz field radiation from the PCA. A huge number of studies have been reported the PCA's performance improvement using a specific nanoplasmonic structure [21–26]. To mention a few, an array of 3 × 3 logarithmic spiral antenna incorporated with plasmonic contact electrodes have been reported to present more than 50 times enhancement

* Corresponding authors.
E-mail addresses: Kolahdouz@ut.ac.ir (M. Kolahdouz), z.kolahdouzesfahani@tudelft.nl (Z. Kolahdouz).

https://doi.org/10.1016/j.optlastec.2019.105726
Received 10 May 2019; Received in revised form 27 July 2019; Accepted 29 July 2019
Available online 03 August 2019

compared to a conventional PCA without antireflection coating (ARC) [27]. This structure benefited from nanoscale carrier transport path lengths that results in better photocarrier collection. In another study, nano-spaced plasmonic contact electrodes were proposed to collect sub-picosecond photocarrier. This structure showed 40 times response compared to a PCA with a non-textured GaAs surface [28]. Another group have introduced a PCA with three-dimensional plasmonic contacts electrodes which achieved THz conversion efficiency of 7.5% [29]. Using three-dimensional plasmonic contact electrodes, the majority of photocarriers can be generated within nanoscale distances from the contact electrodes and drifted to the radiating antenna in a sub-picosecond time-scale. In all of these studies, nanoscale spacing of the electrodes limited the applied DC voltage to avoid breakdown of the LT-GaAs [30]. In an alternative research, optical nanoantennas have been located in the gap of PCA electrodes to overcome the DC applied voltage limitation [31]. In another research, the combination of plasmonic nanodisks, a 120-nm LT-GaAs thin-film, and a bottom-located bowtie antenna has been proposed and resulted in 4.8 higher THz field radiation compared to a conventional PCA with 120 nm LT-GaAs layer [32]. The problem of this work is the complexity of fabrication that causes higher fabrication cost. In other work, array of strip and hexagonal plasmonic nanostructure have been used as an antireflection coating and plasmon exciter which have generated 1.5-fold and 4.2-fold higher terahertz electric field compared to conventional PCA, respectively [33].

In this work, we have proposed an optimized nanodisk array with conventional electrode structure using a simple fabrication method that can enhance the THz radiation more than 5.6 times of the conventional PCA. A simple structure including plasmonic nanodisk array is proposed to obtain a significant terahertz wave radiation from a PCA. The effect of designed nanodisk array's geometrical parameters such as height, diameter and periodicity on the transient photocurrent and generation rates were investigated and optimized using the finite element method (FEM) method. The optimized PCA was fabricated on the LT-GaAs substrates and their THz radiation was measured by time domain spectroscopy set up.

2. Structure design and simulation

The schematic of the conventional PCA and the proposed structures are illustrated in Fig. 1a to 1d showing the defined structural parameters. An LT-GaAs layer with 2 µm thickness on the semi-insulating GaAs (SI-GaAs) was used as the substrate. Dipole antenna electrodes are 20/200 nm thick Ti/Au which are separated by 10 µm gap. In the proposed structure (Fig. 1c), an array of Ti/Au nanodisks is located in the PCA gap between the two electrodes. A 200 nm Si3N4 antireflection coating (ARC) has been used to reduce the reflection of

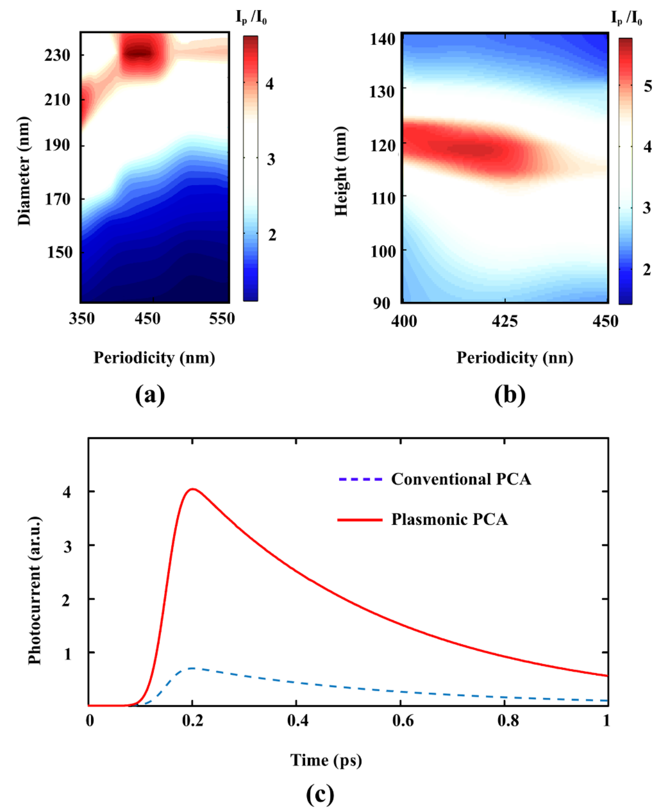

Fig. 2. (a) Distribution of plasmonic PCA photocurrent as a function of nanodisks periodicity (P) and Diameter (D) at nanodisk height of H = 100 nm (b) Distribution of plasmonic PCA photocurrent as a function of nanodisks periodicity (P) and height (H) at nanograting width of D = 230 nm (c) Photocurrent of plasmonic PCA in comparison with conventional PCA.

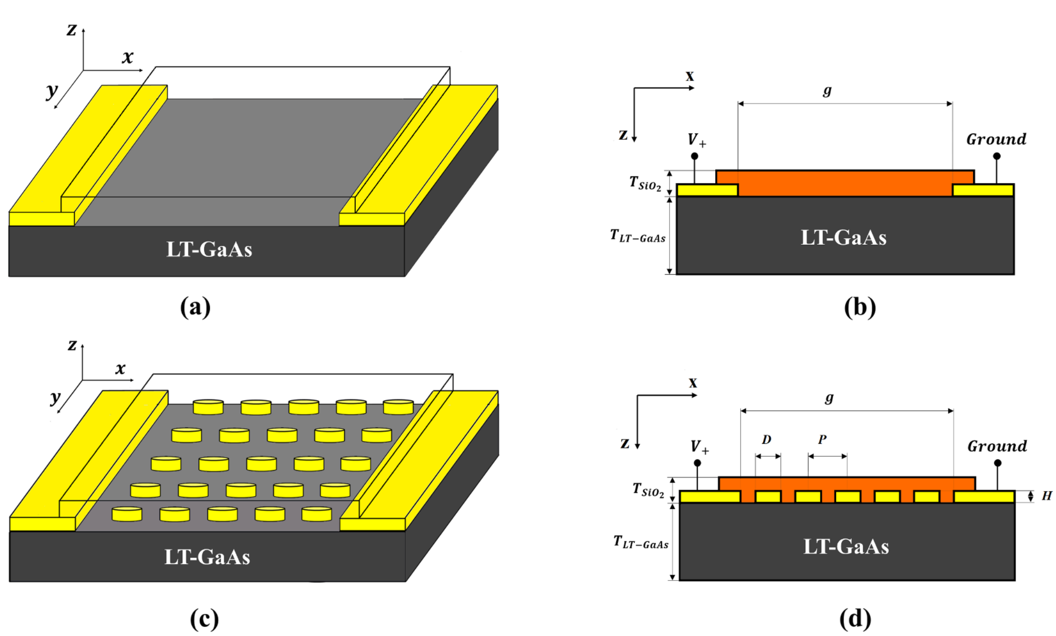

Fig. 1. Schematics of (a, b) the conventional and (c, d) the proposed structure.

laser from LT-GaAs surface. Multiphysics simulations were done in COMSOL 5.2. The FEM method was used to solve the Maxwell's wave equations to investigate the interaction of femtosecond laser pulse with the metallic nanodisk array located in the gap of a PCA. The structure was illuminated from the top surface and the boundary conditions were set to the perfectly matched layers (PMLs) in the propagation direction [22,34,35].

In order to obtain the optimized plasmonic structure, the peak photocurrent enhancement ratio (I_p/I_0) as a function of nanodisk array periodicity (P), diameter (D) and height (H) was investigated. As can be seen in Fig. 2a, the peak photocurrent of plasmonic PCA experiences almost 5-fold enhancement compared to conventional PCA at P = 450 nm and H = 230 nm. In the next step, the diameter was set to 230 nm, which is the optimum point obtained from last step. According to Fig. 2b, the highest enhancement ratio of 6-fold is achieved at P = 420 nm and H = 120 nm. Using optimized plasmonic structure, results in plasmonic mode excitation between two adjacent nanodisk, and so the strong local electric field appears inside the LT-GaAs layer. This will lead to the electron-hole pair generation rate enhancement (Fig. 2c). The time dependent carrier generation rate (G) is obtained as followed (each photon that absorbed by the photoconductive layer generates an electron-hole pair):

$$G(x, y, z, t) = (4\pi k_{PC}/hc)P_s(x, y, z)\exp\left(4\ln(0.5)\frac{(t-t_o)^2}{D_t^2}\right) \quad (1)$$

where k_{PC} is the imaginary part of refractive index, c is the speed of light, D_t is laser pulse duration, h is Planck's constant and $P_s(x, y, z)$ is total power flux density that can be obtained by Maxwell's equation solving. In the next step, transient photocurrent is calculated by combining the calculated generation rate with semiconductor device equation (Poisson equation, drift-diffusion and continuity equation). As can be interpreted by Eq. (1), by enhancing the power flux density inside the LT-GaAs Layer, the generation rate will increase and so, the transient photocurrent.

Moreover, energy and momentum conservation has to be satisfied between incident photons and plasmonic nanostructure for sake of optimum coupling of electromagnetic field to the structure and surface plasmon polariton excitement [36]:

$$K_{sp} = k_{in}\sin\theta \pm mk_g \quad (2)$$

$$k_g = 2\pi/p \quad (3)$$

$$k_{sp} = \frac{2\pi}{\lambda}\sqrt{\frac{\varepsilon_d\varepsilon_m}{\varepsilon_d+\varepsilon_m}} \quad (4)$$

At equations (2)–(4), k_{sp} is the surface plasmons wave vector, θ is the incident electromagnetic wave angle with surface, m is an integer that indicates mode number, k_g is the nanostructure wave vector, p is the periodicity of nanostructure array, ε_m is the relative permittivity of metal and ε_d is the relative permittivity of dielectric. By assuming the normal incident ($\theta = 0$) and substituting Eq. (2) and (3) in Eq. (4), Eq. (4) will be reduce to Eq. (5) as followed:

$$p = \alpha\lambda\left(\sqrt{\frac{\varepsilon_d\varepsilon_m}{\varepsilon_d+\varepsilon_m}}\right)^{-1} \quad (5)$$

where α (mode number) defined as 1, 2, 3 and etc., due to the periodicity of structure.

The scattering cross section as a function of wavelength for different diameter of nanodisks is shown in Fig. 3. According to the results, the peak of scattering cross section shifts to higher wavelength by increasing the dimeter of nanodisks. Higher scattering cross section results in more optical wave scattering in to the LT-GaAs layer by the nanodisks and so the optical path of 800 nm femto-laser pulse inside the photosensitive layer will increase and results in electron-hole generation rate enhancement. Higher rate of photocarrier generation causes more transient photocurrent and so, terahertz wave radiation.

The PCA acquiring the optimized nanodisks array displayed 38.2% absorption efficiency enhancement comparing to the conventional one (see Fig. 4a). Two different views of the E-field around the designed nanodisks are drawn in Fig. 4b and c. Interestingly, the E-field distributions in both figures confirm the enhanced E-fields especially around the metal nanodisks. This confirms that the laser irradiation was trapped between them that led to a high absorption efficiency and finally this high absorption efficiency confirms the photocurrent data discussed earlier [37].

3. Fabrication and experimental measurement

After optimizing the geometrical parameters of the designed nanodisk array, it was time to check the sanity of the results by fabricating PCAs with the designed nanoplasmonic pattern in their gap. To fabricate this device, first, LT-GaAs wafers, from BATOP Company, were cleaned using a standard process. Thereafter, the fabrication process began with patterning the array of Ti/Au nanodisks using electron beam lithography, followed by Ti/Au (5/120 nm) evaporation. Next, using lift-off process in acetone, everything except the nanodisk array was washed off the wafer. Later, the dipole antenna was fabricated using Lift-off process but this time by aligned photolithography followed by Ti/Au (20/200 nm) sputtering. A 200 nm Si3N4 as an ARC, passivation and isolation layer, was deposited using plasma enhanced chemical vapor deposition. In the last step, the nitride layer was etched away chemically from the PCA's bias pads in order to have access to the electrodes. The fabricated dipole antenna gap, width and length were 10 µm, 10 µm and 40 µm, respectively.

The devices were then mounted on the hyper-hemispherical silicon lens and the characteristics of PCAs were investigated using THz time domain spectroscopy method (THz-TDS). In order to compare the performance of our proposed structure, a conventional PCA was also fabricated as a reference.

Field emission scanning electron microscopy (FESEM) images of the fabricated PCAs with the designed array of metallic nanodisks are demonstrated in Fig. 5a and b. The fabricated nanodisks' height, diameter and the array's periodicity were 120 nm, 230 nm and 420 nm, respectively. The dipole antenna gap, width and length were 10 µm, 10 µm and 40 µm, respectively.

Fig. 6a shows the schematic of THz-TDS experimental setup (A pump-probe THz measurement kit from TeTechS Inc.). A TM-polarized 800 nm fiber laser with 100 fs pulse width, repetition rate of 80 MHz and average power of 14 mW on emitter side and 10 mW on receiver side was used as an optical source. In order to achieve the highest THz signal, the fs laser was tightly focused upon the dipole and the ± 10 V square wave was applied between the antenna electrodes. Our PCA with nanoplasmonic structure was used as an emitter and a commercial dipole PCA with 5 µm gap and 20 µm length from TeTechS Inc. employed as the receiver. To compare the performance of our proposed structure, a conventional PCA with antenna gap of 10 µm, width of 10 µm, length of 40 µm, and 200 nm Si3N4 ARC layer was also fabricated as a reference transmitter.

The radiated electric field in time domain and the power in frequency domain for both the reference and the proposed PCAs are illustrated in Fig. 6b and c, respectively. As expected, the THz electric field peak of the nanoplasmonic PCA shows 5.6 times enhancement compared to the reference PCA (see Fig. 6b and c). This can be clarified by the fact that the designed array results in plasmon excitement leading to high local fields near the surface. Higher local field results in more electron-hole generation. Thus, the transient photocurrent increases between electrodes of dipole antenna in the PCA gap. Finally, higher photocurrent persuades THz field radiation enhancement. THz power spectrum of both antennas are displayed in Fig. 6c. It is observed that THz waves with the spectral range between 0.1 and 2.5 THz and the dynamic range of 70 dB were successfully obtained using 800 nm fs

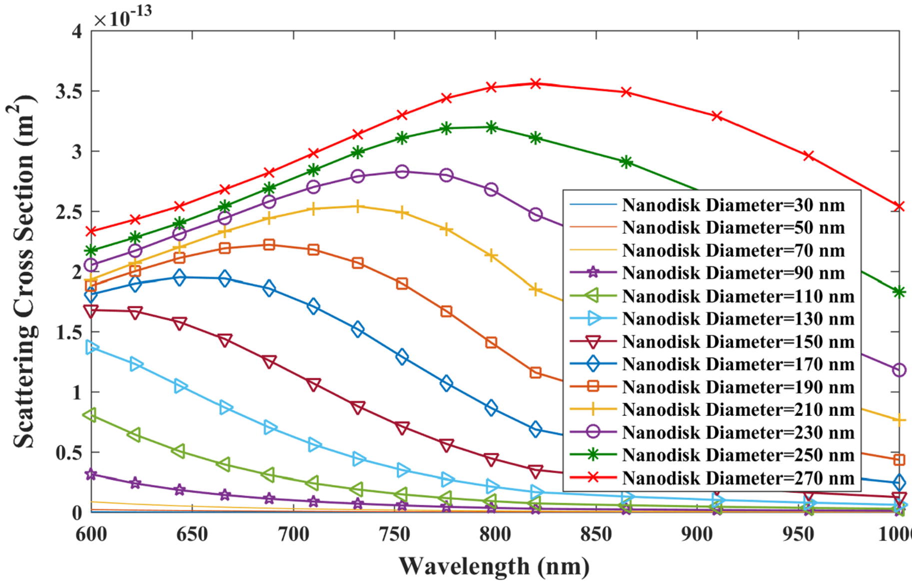

Fig. 3. Scattering cross section of nanodisks as a function of wavelength for different diameter.

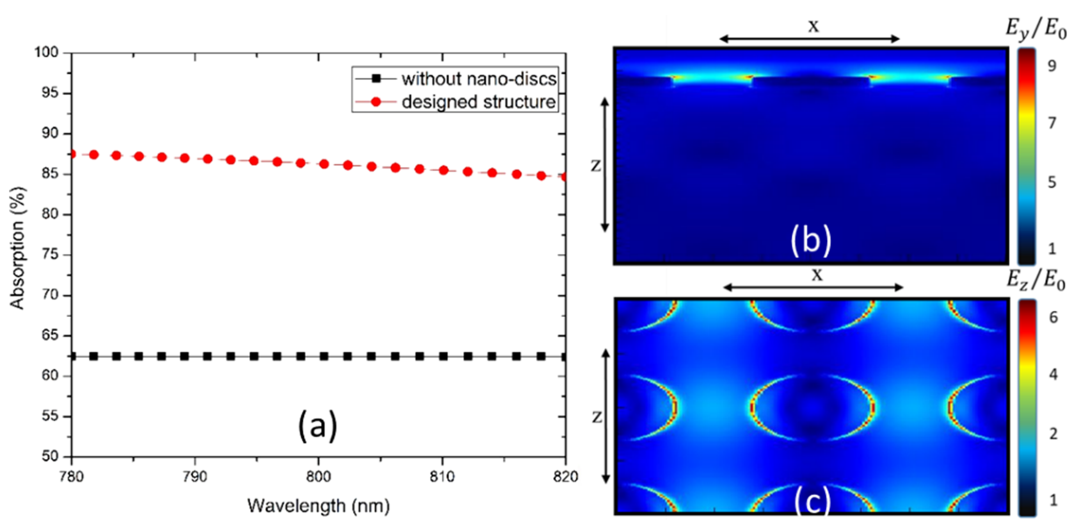

Fig. 4. (a) The absorption efficiency of the antenna with and without nanodisk, (b) side view of the E-field distribution, and (c) top view of the E-field distribution.

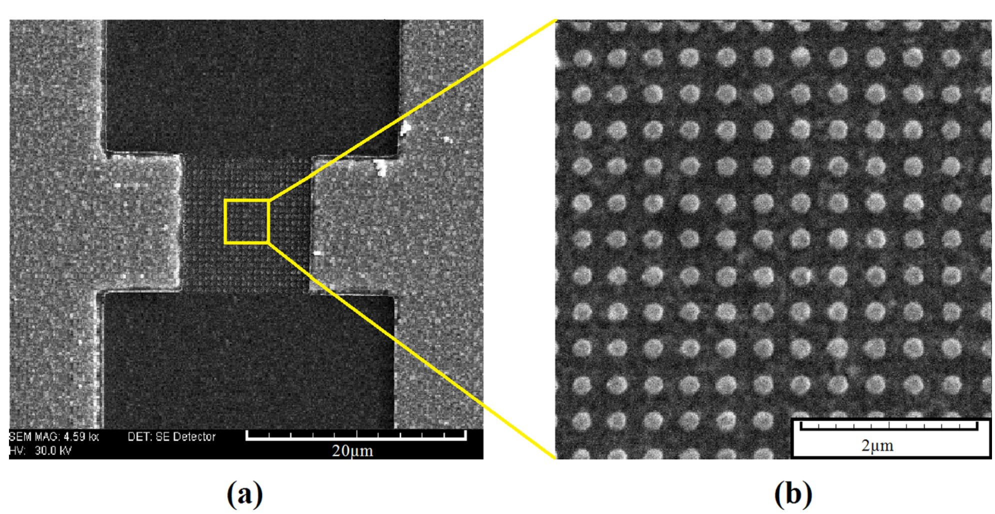

Fig. 5. (a) SEM image of the dipole PCA with the nanodisk array (b) a magnified image of the Ti/Au nanodisk array.

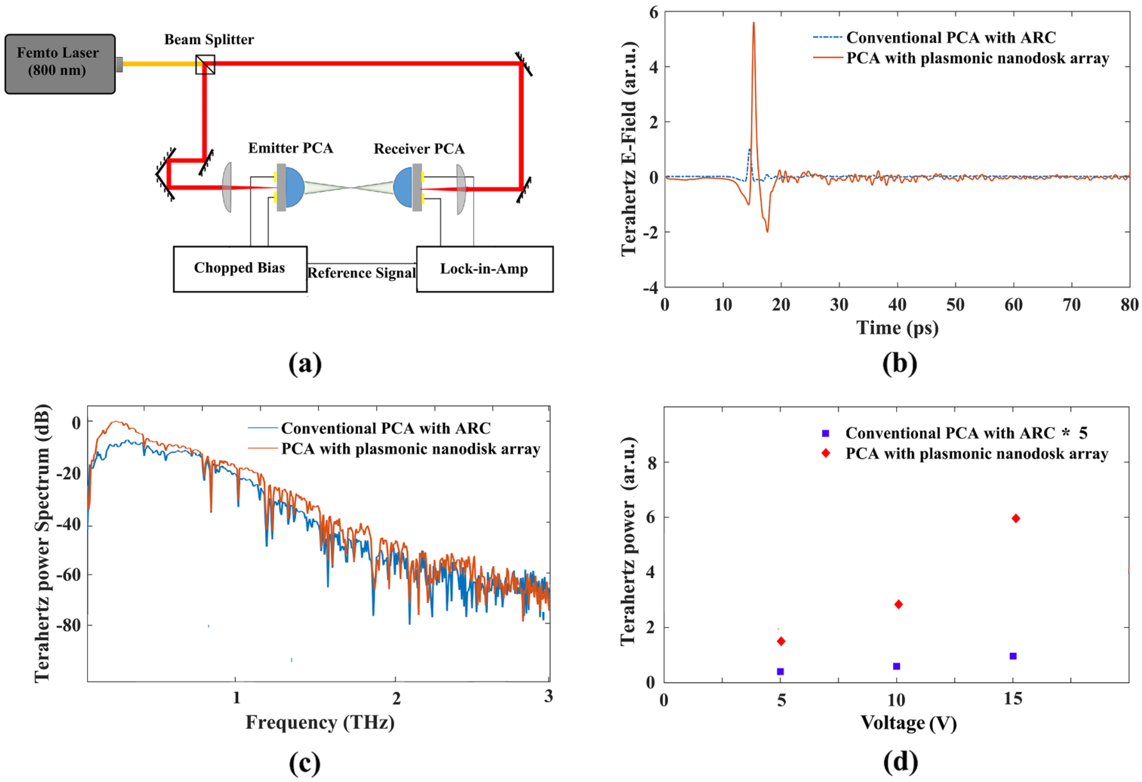

Fig. 6. (a) The schematic of the experimental setup for measuring THz generation using an 800 nm fs laser (b) THz E-Field as a function of time and (c) THz radiation power comparison of a PCA with ARC and a similar PCA with nanoplasmonic structure and (d) Power trends vs bias for PCA with optimized plasmonic structure (red) and conventional PCA with ARC (blue). (For interpretation of the references to colour in this figure legend, the reader is referred to the web version of this article.)

laser. The generated THz power with/without nanodisk array under the 14 mW laser power are plotted as a function of the PCA bias in Fig. 6d. As can be seen in Fig. 6d, enhancement of the applied bias results in significant amplification of THz power.

4. Conclusion

In summary, we presented a plasmonic THz PCA consisting an array of Ti/Au nanodisks in the antenna gap. The proposed structure was primarily simulated using finite difference time domain method and all geometrical parameters (nanodisks' height, diameter and periodicity) were optimized to reach highest electron-hole generation. The introduced plasmonic PCA takes advantage of the enhanced quantum efficiency enabled by the local field enhancement because of plasmon excitation. Thus, the finalized PCA was fabricated on LT-GaAs layer using conventional semiconductor device fabrication methods. Experimental measurements showed that, using array of optimized nanodisks results in more than 5.6 times higher electric field radiation compared to the conventional PCA. This large THz field enhancement demonstrates the potential of the designed structure for improving the optical-to-terahertz conversion efficiency of THz PCAs.

Acknowledgments

The authors would like to acknowledge the TeTechS Inc. from Canada for the test set up and IRAN National Science Foundation for financial support.

References

[1] P.R. Smith, D.H. Auston, M.C. Nuss, Subpicosecond photoconducting dipole antennas, IEEE J. Quantum Electron. 24 (1988) 255–260.
[2] N.M. Burford, M.O. El-Shenawee, Review of terahertz photoconductive antenna technology, Opt. Eng. 56 (2017) 10901.
[3] S. Matsuura, M. Tani, K. Sakai, Generation of coherent terahertz radiation by photomixing in dipole photoconductive antennas, Appl. Phys. Lett. 70 (1997) 559–561.
[4] M. Tonouchi, Cutting-edge terahertz technology, Nat. Photonics. 1 (2007) 97–105, https://doi.org/10.1038/nphoton.2007.3.
[5] N. Khiabani, Y. Huang, Y.-C. Shen, S. Boyes, Theoretical modeling of a photoconductive antenna in a terahertz pulsed system, IEEE Trans. Antennas Propag. 61 (2013) 1538–1546.
[6] M. Bashirpour, S. Ghorbani, M. Kolahdouz, M. Neshat, M. Masnadi-Shirazi, H. Aghababa, Significant performance improvement of a terahertz photoconductive antenna using a hybrid structure, RSC Adv. 7 (2017) 53010–53017.
[7] J. Shi, Z. Li, D.K. Sang, Y. Xiang, J. Li, S. Zhang, H. Zhang, THz photonics in two dimensional materials and metamaterials: properties, devices and prospects, J. Mater. Chem. C. 6 (2018) 1291–1306.
[8] H. Zhang, J.K. Wahlstrand, S.B. Choi, S.T. Cundiff, Contactless photoconductive terahertz generation, Opt. Lett. 36 (2011) 223–225.
[9] A. Bockelt, J. Palací, B. Vidal, Control of terahertz emission in photoconductive antennas through an additional optical continuous wave, Opt. Lett. 38 (2013) 3123–3125.
[10] W. Ye, R. Long, H. Huang, Y. Xiong, Plasmonic nanostructures in solar energy conversion, J. Mater. Chem. C. 5 (2017) 1008–1021.
[11] S. Lepeshov, A. Gorodetsky, A. Krasnok, E. Rafailov, P. Belov, Enhancement of terahertz photoconductive antenna operation by optical nanoantennas, Laser Photonics Rev. 11 (2017) 1–21, https://doi.org/10.1002/lpor.201600199.
[12] C.W. Berry, M. Jarrahi, Terahertz generation using plasmonic photoconductive gratings, New J. Phys. 14 (2012) 105029.
[13] X. Yang, A. Vorobiev, A. Generalov, M.A. Andersson, J. Stake, A flexible graphene terahertz detector, Appl. Phys. Lett. 111 (2017) 2–6, https://doi.org/10.1063/1.4993434.
[14] M. Bashirpour, M. Forouzmehr, S.E. Hosseininejad, M. Kolahdouz, M. Neshat, Improvement of terahertz photoconductive antenna using optical antenna array of ZnO nanorods, Sci. Rep. 9 (2019) 1414, https://doi.org/10.1038/s41598-019-38820-3.
[15] M. Pu, X. Ma, X. Li, Y. Guo, X. Luo, Merging plasmonics and metamaterials by two-dimensional subwavelength structures, J. Mater. Chem. C. 5 (2017) 4361–4378.
[16] J. Poursafar, M. Bashirpour, M. Kolahdouz, A.V. Takaloo, M. Masnadi-Shirazi, E. Asl-Soleimani, Ultrathin solar cells with Ag meta-material nanostructure for light absorption enhancement, Sol. Energy. 166 (2018) 98–102.
[17] K.Q. Le, J. Bai, Q.M. Ngo, P.-Y. Chen, Fabrication and numerical characterization of infrared metamaterial absorbers for refractometric biosensors, J. Electron. Mater. 46 (2017) 668–676.
[18] K.Q. Le, Q.M. Ngo, T.K. Nguyen, Nanostructured metal–insulator–metal metamaterials for refractive index biosensing applications: design, fabrication, and

characterization, IEEE J. Sel. Top. Quantum Electron. 23 (2016) 388–393.
[19] K.Q. Le, S.T.K. Ho, N.T.H. Tran, Q.M. Ngo, H.P.T. Nguyen, Observation of Fano-like resonance in dual-blade shaped gold nanostructures, J. Phys. D. Appl. Phys. 52 (2018) 45106.
[20] S. Ghorbani, M. Bashipour, M. Kolahdouz, Improving unbiased terahertz photoconductive antenna based on dissimilar schottky barriers using plasmonic mode excitation, Optik (Stuttg) (2019) 162975.
[21] S. Ghorbani, M. Bashirpour, J. Poursafar, M. Kolahdouz, M. Neshat, A. Valinejad, Thin film tandem nanoplasmonic photoconductive antenna for high performance terahertz detection, Superlattices Microstruct. (2018).
[22] M. Bashirpour, M. Kolahdouz, M. Neshat, Enhancement of optical absorption in LT-GaAs by double layer nanoplasmonic array in photoconductive antenna, Vacuum 146 (2017) 430–436, https://doi.org/10.1016/j.vacuum.2017.07.035.
[23] S.-G. Park, Y. Choi, Y.-J. Oh, K.-H. Jeong, Terahertz photoconductive antenna with metal nanoislands, Opt. Express 20 (2012) 25530–25535.
[24] C.W. Berry, M.R. Hashemi, M. Jarrahi, Generation of high power pulsed terahertz radiation using a plasmonic photoconductive emitter array with logarithmic spiral antennas, Appl. Phys. Lett. 104 (2014) 081122, https://doi.org/10.1063/1.4866807.
[25] F. Fesharaki, A. Jooshesh, V. Bahrami-Yekta, M. Mahtab, T. Tiedje, T.E. Darcie, R. Gordon, Plasmonic antireflection coating for photoconductive terahertz generation, ACS Photonics 4 (2017) 1350–1354, https://doi.org/10.1021/acsphotonics.7b00410.
[26] S. Ghorbani, M. Bashirpour, M. Forouzmehr, M.R. Kolahdouz, M. Neshat, Simulation of THz photoconductive antennas loaded by different metallic nanoparticles, in: 2016 Fourth Int. Conf. Millimeter-Wave Terahertz Technol., 2016: pp. 62–64. https://doi.org/10.1109/MMWaTT.2016.7869917.
[27] C.W. Berry, N. Wang, M.R. Hashemi, M. Unlu, M. Jarrahi, Significant performance enhancement in photoconductive terahertz optoelectronics by incorporating plasmonic contact electrodes, Nat. Commun. 4 (2013) 1622, https://doi.org/10.1038/ncomms2638.
[28] B. Heshmat, H. Pahlevaninezhad, Y. Pang, M. Masnadi-Shirazi, R. Burton Lewis, T. Tiedje, R. Gordon, T.E. Darcie, Nanoplasmonic terahertz photoconductive switch on GaAs, Nano Lett. 12 (2012) 6255–6259.
[29] S. Yang, M.R. Hashemi, C.W. Berry, M. Jarrahi, 7.5% optical-to-terahertz conversion efficiency offered by photoconductive emitters with three-dimensional contact plasmonic electrodes, IEEE Trans. Terahertz Sci. Technol. (2014) 1–7.
[30] S. Lepeshov, A. Gorodetsky, A. Krasnok, N. Toropov, T.A. Vartanyan, P. Belov, A. Alú, E.U. Rafailov, Boosting terahertz photoconductive antenna performance with optimised plasmonic nanostructures, Sci. Rep. 8 (2018) 6624, https://doi.org/10.1038/s41598-018-25013-7.
[31] O. Mitrofanov, I. Brener, T.S. Luk, J.L. Reno, Photoconductive terahertz near-field detector with a hybrid nanoantenna array cavity, ACS Photonics (2015), https://doi.org/10.1021/acsphotonics.5b00475 acsphotonics.5b00475.
[32] N.M. Burford, M.J. Evans, M.O. El-Shenawee, Plasmonic nanodisk thin-film terahertz photoconductive antenna, IEEE Trans. Terahertz Sci. Technol. 8 (2018) 237–247, https://doi.org/10.1109/TTHZ.2017.2782484.
[33] A. Jooshesh, L. Smith, M. Masnadi-Shirazi, V. Bahrami-Yekta, T. Tiedje, T.E. Darcie, R. Gordon, Nanoplasmonics enhanced terahertz sources, Opt. Express. 22 (2014) 27992–28001.
[34] M.A. Awal, Z. Ahmed, M.A. Talukder, An efficient plasmonic photovoltaic structure using silicon strip-loaded geometry, J. Appl. Phys. 117 (2015), https://doi.org/10.1063/1.4907873.
[35] M. Shaban, J. Poostforooshan, A.P. Weber, Surface-initiated polymerization on unmodified inorganic semiconductor nanoparticles via surfactant-free aerosol-based synthesis toward core-shell nanohybrids with a tunable shell thickness, J. Mater. Chem. A. 5 (2017) 18651–18663, https://doi.org/10.1039/C7TA04985D.
[36] P. Karpinski, A. Miniewicz, Surface plasmon polariton excitation in metallic layer via surface relief gratings in photoactive polymer studied by the finite-difference time-domain method, Plasmonics 6 (2011) 541–546, https://doi.org/10.1007/s11468-011-9234-3.
[37] J. Poursafar, M. Kolahdouz, E. Asl Soleimani, S. Golmohammadi, Ultra-thin tandem-plasmonic photovoltaic structures for synergistically enhanced light absorption, RSC Adv. (2016), https://doi.org/10.1039/C6RA06586D.